Synthesis and Structure of $n = 5$ Member of the $A_{n+1}Mn_nO_{3n+3}(A_2O)$ Series

Lijian Bie,[†] Yingxia Wang,[†] Jianhua Lin,*[,†] Chun-K. Loong,[‡] J. W. Richardson, Jr.,[‡] Liping You,[§] and Cheng Dong[||]

The State Key Laboratory for Rare Earth Materials Chemistry and Applications, College of Chemistry and Molecular Engineering, Peking University, Beijing 100871, P. R. China, Intense Pulsed Neutron Source Division, Argonne National Laboratory, Argonne, Illinois 60439, Electron Microscopy Laboratory, Department of Physics, Peking University, Beijing 100871, P. R. China, and Institute of Physics, Chinese Academy of Sciences, Beijing 100080, P. R. China

Received July 1, 2002. Revised Manuscript Received November 15, 2002

$La_4Ba_{2.6}Ca_{1.4}(Mn_4Ca)O_{19}$, a novel hexagonal perovskite-intergrowth manganate, was synthesized by solid-state reaction. It crystallizes in the space group $C2/m$ (no. 12) with the lattice parameters of $a = 9.8394(4)$ Å, $b = 5.6823(2)$ Å, $c = 15.6435(3)$ Å, and $\beta = 102.093(5)$, cell volume of 855.21(5) Å^3, and $Z = 2$. The structure was investigated by electron, X-ray, and neutron diffraction techniques and fully resolved by refinements of both X-ray and neutron powder diffraction data. The structure can be described as alternate stacking of 6H-type hexagonal perovskite blocks and graphite-like Ca_2O sheets. In the hexagonal perovskite block, Mn and Ca cations occupy the octahedral sites of the corner-shearing and face-shearing octahedra, respectively. Preferred La/Ba and Ca/La substitution at the ratio of 7:3 was observed over specific crystallographic sites. $La_4Ba_{2.6}Ca_{1.4}(Mn_4Ca)O_{19}$ is an $n = 5$ member of the $A_{n+1}Mn_nO_{3n+3}(Ca_2O)$ series in which $^1/_5$ of the Mn atoms in the 6H-hexagonal perovskite blocks are replaced by Ca. A structural principle that is based on alternate stacking of close-packed $[AO_3]$ layers and graphite-like sheets is introduced for structural prediction of new hexagonal perovskite intergrowth compounds.

Introduction

The study of compounds whose structures are built up by stacking of layers derived from perovskite is one of the most interesting and well-recognized research fields in solid-state sciences. Many fascinating physical properties, such as high-Tc superconductivity[1] and colossal magnetoresistivity,[2] were found primarily in these compounds. Most of these compounds are built up from tetragonal perovskite layers, i.e., the (001) plane of the cubic perovskite. Among them, the Ruddlesden−Popper phase $(ABO_3)_nAO$[3] is one interesting family in which multiple tetragonal perovskite layers of *n*-octahedron thick alternate with rock-salt layers. One crucial factor for the formation of this structural type is the identical (001) planes exhibited by cubic perovskite and rock salt structures, so that the topology of the interfacial structure remains unchanged or undergoes only a small distortion when they form an intergrowth compound. Similarly, the hexagonal perovskite layers, which can be derived from either the (111) plane of the cubic perovskite or the (001) plane of the $BaNiO_3$-type structure, may also serve as fundamental structural elements in conjunction with another compatible layer structure to generate various hexagonal perovskite intergrowth compounds. One example is the $(A_3A'BO_6)_\alpha$-$(ABO_3)_{3\beta}$ phase in which different one-dimensional chain structures are formed by stacking octahedra and trigonal prisms in ordered sequences.[4] Recently, several new compounds belonging to a hexagonal perovskite intergrowth family of $A_{n+1}B_nO_{3n+3}(A'_2O)$ were identified in manganate and ruthenate systems.[5−8] Their structures

* Corresponding author. E-mail: jhlin@chem.pku.edu.cn. Telephone: +86 10 62751715. Fax: +86 10 62751708.

[†] The State Key Laboratory for Rare Earth Materials Chemistry and Applications.

[‡] Argonne National Laboratory.

[§] Electron Microscopy Laboratory, Peking University.

[||] Chinese Academy of Sciences.

(1) Bednorz, J. G.; Muller, K. A. *J. Phys.* **1986**, *B64*, 189. Otzschi, K. D.; Poeppelmeier, K. R.; Salvador, P. A.; Mason, T. O.; Sinkler, W.; Zhang, H.; Marks, L. D. *Physica C* **1997**, *282−287*, 837. Attfield, J. P.; Kharlanov, A. L.; McAllister, J. A. *Nature*, **1998**, *394*, 157. Orenstein, J.; Millis, A. J. *Science* **2000**, *288*, 468. He, T.; Huang, Q.; Ramirez, A. P.; Wang, Y.; Regan, K. A.; Rogado, N.; Hayward, M. A.; Haas, M. K.; Slusky, J. S.; Inumara, K.; Zandbergen, H. W.; Ong, N. P.; Cava, R. J. *Nature* **2001**, *411*, 53.

(2) Rao, C. N. R.; Cheetham, A. K.; Mahesh, R. *Chem. Mater.* **1996**, *8*, 2421. Majumdar, P.; Littlewood, P. B. *Nature* **1998**, *395*, 479. Kobayashi, K.-I.; Kimura, T.; Sawada, H.; Terakura, K.; Tokura, Y. *Nature* **1998**, *395*, 677. Ramirez, A. P.; Subramanian, M. A. *Science*, **1997**, *277*, 546.

(3) Hyde, G. B.; Andersson, S. *Inorganic Crystal Structures*; John Wiley & Sons: New York, 1989. Rao, C. N. R.; Raveau, B. *Transition Metal Oxides*, 2nd edition; Wiley-VCH: New York, 1998; p 61. Battle, P. D.; Branford, W. R.; Mihut, A.; Rosseinsky, M. J.; Singleton, J.; Sloan, J.; Spring, L. E.; Vente, J. F. *Chem. Mater.* **1999**, *11*, 674.

(4) Boulahya, K.; Parras, M.; Gonzalez-Calbet, J. M. *Chem. Mater.* **2000**, *12*, 25. Boulahya, K.; Amador, U.; Parras, M.; Gonzalez-Calbet, J. M. *Chem. Mater.* **2000**, *12*, 966. Boulahya, K.; Parras, M.; Gonzalez-Calbet, J. M.; *Chem. Mater.* **2000**, *12*, 2727.

(5) Wang, Y. X.; Lin, J. H.; Du, Y.; Qin, R. W.; Han, B.; Loong, C. K. *Angew. Chem.* **2000**, *112*, 2842, *Angew. Chem., Int. Ed.* **2000**, *39*, 2739.

(6) Wang, Y. X.; Bie, L. J.; Du, Y.; Lin, J. H.; Loong, C. K.; You, L. P. *J. Solid State Chem.* accepted for publication.

(7) Bie, L. J.; Lin, J. H.; Wang, Y. X.; Loong, C. K.; You, L. P. *Inorg. Chem. Commun.* **2002**, *5*, 966.

10.1021/cm020706n CCC: $25.00 © 2003 American Chemical Society
Published on Web 12/24/2002

are built up by alternative stacking of the hexagonal perovskite blocks and the graphite-like [Ca_2O] sheets. For example, the $n = 1$ members, $Ln_2Ca_2MnO_7$ (Ln = La, Nd, Sm),[5,6] comprise single hexagonal perovskite blocks [Ln_2MnO_6] and graphite-like sheets [Ca_2O], and likewise the $n = 2$ members, $La_2Ba_{0.8}Sr_{0.6}Ca_{1.6}Mn_2O_{10}$[7] and $Ba_5Ru_2O_{10}$,[8] comprise 2H-hexagonal perovskite blocks and graphite like sheets. In this paper, we report the synthesis and crystal structure of a new compound, $La_4Ba_{2.6}Ca_{1.4}(Mn_4Ca)O_{19}$, which can be considered as the $n = 5$ member in the $A_{n+1}Mn_nO_{3n+3}(Ca_2O)$ family with one-fifth of the Mn replaced by Ca.

Experimental Section

Polycrystalline samples were synthesized by a high-temperature solid-state reaction. To effectuate a complete reaction, we first prepared oxide precursors by thermal decomposition of the mixed citrates. In the case of preparing $La_4Ba_{2.6}Ca_{1.4}(Mn_4Ca)O_{19}$, excess citric acid was added, under stirring, to an aqueous solution containing stoichiometric, commercial-grade $La(NO_3)_3$, $Ba(NO_3)_2$, $Ca(NO_3)_2$, and $Mn(NO_3)_2$. Rare earth oxides are 99.99% pure, and alkaline earth and manganese nitrates are of analytical grade. The solution was evaporated on a heat plate to remove water. The obtained solid mixture was heated at 800 °C in a furnace, yielding a fine powder of a mixed oxide precursor. The powder was then compacted and sintered at 1100 °C in an alumina crucible in air for 3−5 days. After repeated grinding, pressing, and heating, a polycrystalline powder of $La_4Ba_{2.6}Ca_{2.4}Mn_4O_{19}$ was obtained. Samples of various nominal compositions were prepared by this method. An oxidation state of 4.02(2) for manganese in $La_4Ba_{2.6}Ca_{1.4}(Mn_4Ca)O_{19}$ was determined by an oxalate titration method.

X-ray powder-diffraction data were recorded in $\theta-2\theta$ scans ($10 < 2\theta < 120°$, step size 0.02°, counting time 5 s per step) on a Rigaku D/Max-2000 diffractometer using a Cu Kα radiation with a graphite secondary monochromator. Neutron diffraction was conducted using the general purpose power diffractometer at the Intense Pulsed Neutron Source of Argonne National Laboratory. Electron diffraction was carried out on a Hitachi H-9000 electron microscope (300 kV). Magnetic susceptibility was measured using an Oxford Maglab-2000 magnetometer at a field of 0.5 T between 5 and 300 K. The magnetization curves at 10, 20 and 300 K were measured with a Quantum Design SQUID. AC impedance data were obtained from an HP4192A impedance analyzer in a frequency range of 5 Hz−12 MHz and a temperature range of 20−680 °C; two faces of the pressed sample were pasted with Pt paster.

Results

Evidence for the presence of $La_4Ba_{2.6}Ca_{1.4}(Mn_4Ca)O_{19}$ emerged during a systematic search for $n = 2$ members in the $A_{n+1}Mn_nO_{3n+3}(Ca_2O)$ series. Initially, a sample with nominal composition of $La_2BaCa_2Mn_2O_{10}$ was found to contain a new phase and its diffraction pattern does not match any known phases (see powder pattern s01 in Figure 1). In an attempt to achieve a single-phase material for $n = 2$, samples containing systematically varied contents of La, Ba, and Ca and constrained to a fixed (La+Ba+Ca)/Mn ratio of 5:2 were synthesized for further studies. Figure 2 shows the nominal compositions of the samples. The X-ray diffraction patterns of selected samples, as shown in Figure 1, indicate that the nominal sample of $La_2Ba_{1.4}Ca_{1.6}Mn_2O_{10}$ is close to single-phase. Subsequent repeated syntheses and structural refinements led to the final composition of $La_4Ba_{2.6}Ca_{2.4}Mn_4O_{19}$ and the confirmation of an $n = 5$ member in the $A_{n+1}Mn_nO_{3n+3}(Ca_2O)$ series of hexagonal perovskite-intergrowth manganates.

Figure 3 shows two electron diffraction patterns of $La_4Ba_{2.6}Ca_{1.4}(Mn_4Ca)O_{19}$ in the [010] and [$\bar{1}$10] zones,

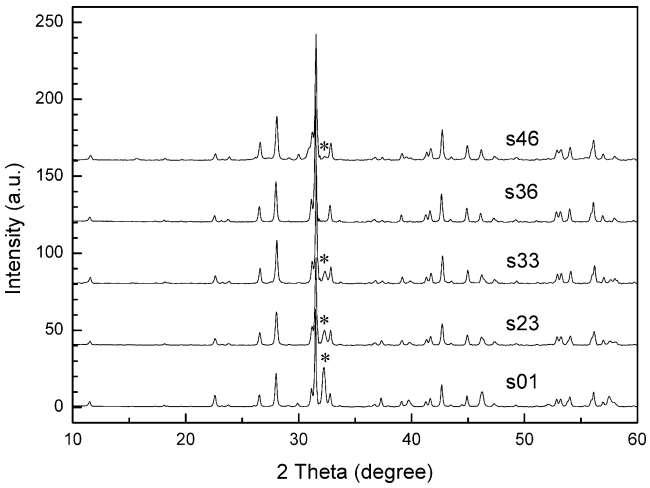

Figure 1. X-ray diffraction patterns of selected samples at room temperature. Nominal compositions of the samples are s01, $La_2BaCa_2Mn_2O_{10}$; s23, $La_2Ba_{1.2}Ca_{1.8}Mn_2O_{10}$; s33, $La_{2.2}Ba_{1.2}Ca_{1.6}Mn_2O_{10}$; s36, $La_2Ba_{1.4}Ca_{1.6}Mn_2O_{10}$; s46, $La_{2.3}Ba_{1.3}Ca_{1.4}Mn_2O_{10}$. The reflections marked with "*" originate from the impurity phases.

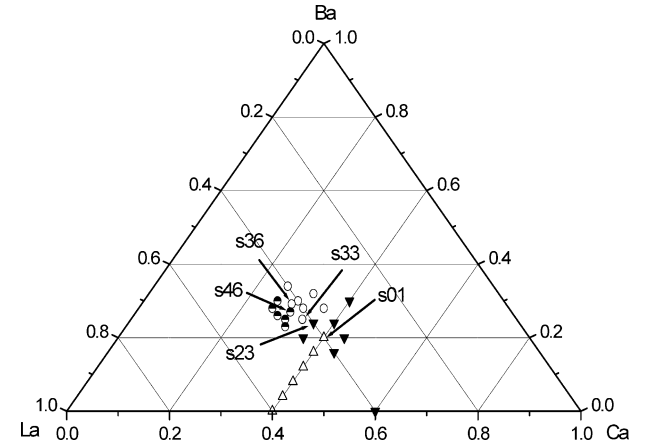

Figure 2. Schematic diagram of the nominal composition of the samples: s01, $La_2BaCa_2Mn_2O_{10}$; s23, $La_2Ba_{1.2}Ca_{1.8}Mn_2O_{10}$; s33, $La_{2.2}Ba_{1.2}Ca_{1.6}Mn_2O_{10}$; s36, $La_2Ba_{1.4}Ca_{1.6}Mn_2O_{10}$; s46, $La_{2.3}Ba_{1.3}Ca_{1.4}Mn_2O_{10}$. The symbols shown in the figure are the sequence number of the samples.

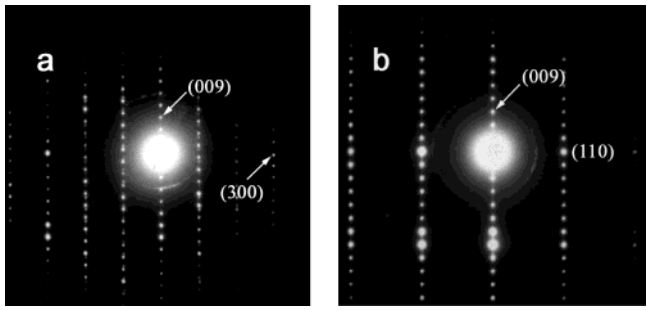

Figure 3. Electron diffraction patterns of $La_4Ba_{2.6}Ca_{1.4}(Mn_4Ca)O_{19}$ in (a) [010], and (b) [$\bar{1}$10] zones. The reflections are indexed according to a rhombohedral cell of $a = 5.68$ and $c = 45.86$ Å.

(8) Grasset, F.; Dussarrat C.; Darriet, J. *J. Mater. Chem.*, **1997**, *7*, 1911. Grasset, F.; Zakhour, M.; Darriet J. *J. Alloys Compd.* **1999**, *287*, 25.

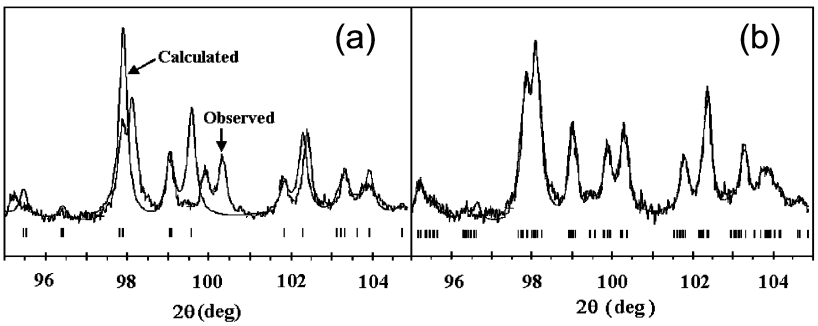

Figure 4. Profile fit of the room-temperature X-ray powder diffraction pattern of $La_4Ba_{2.6}Ca_{1.4}(Mn_4Ca)O_{19}$ to (a) a rhombohedral cell of space group $R\bar{3}m$ and (b) a C-centered monoclinic cell of space group $C2/m$. Only the high-angle portions are shown in this figure.

respectively. The diffraction patterns can be readily indexed by a rhombohedral cell ($a = 5.68$ and $c = 45.86$ Å) of a plausible space group among $R\bar{3}m$, $R3m$, $R32$, $R\bar{3}$, or $R3$. A full X-ray diffraction-profile refinement showed that the rhombohedral cell matches the powder pattern reasonably well up to $2\theta = 90°$ but substantial deviation was observed at higher angles (Figure 4a). Guided by the fact that the diffraction patterns exhibit a pseudo-rhombohedral symmetry, we pursued the real symmetry among the subgroups within the rhombohedral space groups by removing the 3-fold axis from rhombohedral cell, hence resulting in a C-centered monoclinic or a triclinic cell. The C-centered monoclinic cell can be deduced by the following matrix:[9] $a = 2a_R + b_R$, $b = b_R$, and $c = 1/3\,(2a_R + b_R + c_R)$. Such refinement showed that the C-centered monoclinic cell fits the data over the whole range of the diffraction data much better than the case of the rhombohedral cell (see Figure 4b for a comparison at high angles), and consequently was used for further structure determination.

The structure model of $La_4Ba_{2.6}Ca_{1.4}(Mn_4Ca)O_{19}$ was established by first applying a direct method on powder X-ray diffraction data. The individual reflection intensities extracted by EXTRA[10] were used to build a structure model according to Sirpow92[11]. The space group of $C2/m$ with the lattice constants $a = 9.8394(4)$, $b = 5.6823(2)$, $c = 15.6435(3)$ Å, and $\beta = 102.093(5)°$ was obtained. The cation positions and a part of the oxygen positions could be located directly from the E-map. The rest of the oxygen positions were determined by subsequent difference Fourier analysis during the Rietveld refinement (GSAS)[12] on both the X-ray and neutron diffraction data. The structure refinements indicated partial occupation of the O7 and O8 sites and mutual substitution at some cation positions. The occupation factors of these positions were refined at the initial stage of the refinement, but limited to appropriate values according to reasonable stoichiometry of the compound in the final stage. The crystallographic data, atomic coordinates, and selected bond distances are listed in Tables 1−3. The profile-fit of the neutron diffraction pattern (Rp = 0.054, Rwp = 0.078) is shown in Figure 5. As shown in the figure, the sample contains a considerable amount of CaO (about 5% in volume).

Table 1. Crystallographic Data of $La_4Ba_{2.6}Ca_{1.4}(Mn_4Ca)O_{19}$

structure formula	$La_4Ba_{2.6}Ca_{1.4}(Mn_4Ca)O_{19}$
formula weight	1532.6
crystal system	C-centered monoclinic
space group	$C2/m$ (no. 12)
unit cell	$a = 9.8394(4)$, $b = 5.6823(2)$, $c = 15.6435(3)$ Å, $\beta = 102.093(5)$
V	855.21(5) Å^3
Z	2
density (calculated)	5.896 g/cm^3
diffraction technique	neutron and X-ray diffractions
structure solution	direct method, Extra and Sirpow92
Rietveld refinement	GSAS
R indices	Rp = 0.0354, Rwp = 0.0479 (neutron)
goodness of fit	1.46

The crystal structure of $La_4Ba_{2.6}Ca_{1.4}(Mn_4Ca)O_{19}$, as shown in Figure 6, can be described as alternate stacking of the 6H-hexagonal perovskite blocks[13] and graphite-like Ca_2O sheets. The composition of the 6H-block is $[A_6(Mn_4Ca)O_{18}]$, in which both Mn and Ca cations occupy the octahedral sites between the close-packed $[AO_3]$ arrays. Structural refinements of the neutron diffraction data show unambiguously that the Mn and Ca cations are well ordered: Ca atoms reside in the central octahedra that share all corners with those octahedra occupied by Mn, which are face-sharing in pairs. The ordered distribution of Mn and Ca in the 6H-block is also supported by the fact that the observed M−O bond distances are significantly different in these octahedra. The averaged Ca−O bond distance (2.22 Å) in a Ca-octahedron is significantly larger than that in the Mn-octahedra (1.90 Å). These values are in good agreement with M−O bond distances found in typical compounds with octahedrally coordinated Ca^{2+} and Mn^{4+} ions. Additionally, Table 2 shows the preferred La/Ba and Ca/La substitution at the ratio of 7:3 over the crystallographic sites La1 and Ca1, respectively. Because of the large difference in ionic size (La^{3+}, 1.50 Å; Ba^{2+}, 1.75 Å; for CN = 12[14]) such preferred substitution is corroborated by the average M−O bond distances. The averaged Ba/La−O distance is 2.86 Å (CN = 12) whereas the averaged Ba−O and La−O distances from the pure Ba1 site and pure La2 site are 2.93 Å (CN =

(9) Hahn, T. *International Tables for Crystallography*, Volume A, 3rd ed.; Kluwer Academic Publishers: Norwell, MA, 1992; p 80.

(10) Altomare, A.; Burla, M. C.; Cascarano, G.; Giacovazzo, C.; Guagliardi, A.; Moliterni, A. G. G.; Polidori, G. *J. Appl. Crystallogr.* **1995**, *28*, 842.

(11) Altomare, A.; Burla, M. C.; Camalli, M.; Cascarano, G.; Giacovazzo, C.; Guagliardi, A.; Polidori, G. *J. Appl. Crystallogr.* **1994**, *27*, 435.

(12) Larson, C.; von Dreele, R. B. *Report LAUR 86-748*; Los Alamos National Laboratory: Los Alamos, NM, 1985.

(13) Rao, C. N. R.; Gopalakrishnan, J. *New Directions in Solid State Chemistry*, 2nd ed.; Cambridge University Press: New York, 1997; p 54.

(14) Shannon, R. D. *Acta Crystallogr.* **1976**, *A32*, 751.

Table 2. Refined Atomic Coordinates of $La_4Ba_{2.6}Ca_{1.4}(Mn_4Ca)O_{19}$

atom	site	*x*	*y*	*z*	occupancy ratio	Uiso
La1	4i	0.9327(7)	0.5	0.76921(26)	La/Ba = 0.7/0.3	0.0153(9)
La2	4i	0.5417(6)	0.5	0.64325(20)	1	0.0056(5)
Ba1	4i	0.1302(9)	0	0.91595(31)	1	0.0112(10)
Ca1	4i	0.6660(9)	0	0.48632(25)	Ca/La = 0.7/0.3	0.0101(8)
Ca2	2b	0	0.5	0	1	0.0063(10)
Mn1	4i	0.7218(16)	0	0.6819(4)	1	0.0096(9)
Mn2	4i	0.2109(15)	0	0.1527(4)	1	0.0096(9)
O1	8j	0.1233(6)	0.7431(10)	0.0900(4)	1	0.0215(4)
O2	4i	0.1609(8)	0.5	0.9142(8)	1	0.0215(4)
O3	4i	0.3993(9)	0.5	0.7625(9)	1	0.0215(4)
O4	8j	0.1877(6)	0.7505(11)	0.7618(4)	1	0.0215(4)
O5	4i	0.0550(8)	0.5	0.6167(7)	1	0.0215(4)
O6	8j	0.2436(5)	0.7302(11)	0.3883(4)	1	0.0215(4)
O7	4h	0	0.114(6)	0.5	0.25	0.0215(4)
O8	4i	0.074(4)	0	0.5	0.25	0.0215(4)

Table 3. Selected Bond Distances and Angles of $La_4Ba_{2.6}Ca_{1.4}(Mn_4Ca)O_{19}$

band	mult.	length(Å)	angle	degree(°)
La1−O1	2	2.751(7)	O1−Mn2−O1	103.0(6)
La1−O2	1	2.838(13)	O1−Mn2−O2	89.87(33)
La1−O3	2	2.860(1)	O1−Mn2−O3	95.7(6)
La1−O4	2	2.908(9)	O1−Mn2−O4	171.3(4)
La1−O4	2	2.778(9)	O1−Mn2−O4	84.74(24)
La1−O5	1	2.888(12)	O2−Mn2−O3	171.1(8)
La1−O6	2	3.000(8)	O2−Mn2−O4	94.3(6)
La2−O3	1	2.557(13)	O3−Mn2−O4	79.28(27)
La2−O4	2	2.529(7)	O4−Mn2−O4	87.3(5)
La2−O5	2	2.878(2)	O3−Mn1−O4	80.58(33)
La2−O6	2	2.618(6)	O3−Mn1−O5	175.2(9)
La2−O6	2	3.145(7)	O3−Mn1−O6	97.3(7)
La2−O7[a]	2	2.286(10)	O4−Mn1−O4	92.6(5)
La2−O8[a]	1	2.329(12)	O4−Mn1−O5	96.1(7)
La2−O8[a]	1	2.292(10)	O4−Mn1−O6	174.6(4)
Ba1−O1	2	2.875(11)	O4−Mn1−O6	82.09(23)
Ba1−O1	2	3.103(7)	O5−Mn1−O6	85.7(4)
Ba1−O1	2	2.810(11)	O6−Mn1−O6	103.2(5)
Ba1−O2	2	2.858(1)	O1−Ca2−O1	79.71(30)
Ba1−O2	1	2.999(12)	O1−Ca2−O2	91.11(17)
Ba1−O3	1	2.939(13)	O1−Ca2−O2	88.89(17)
Ba1−O4	2	2.953(8)		
Mn1−O3	1	1.928(16)		
Mn1−O4	2	1.968(8)		
Mn1−O5	1	1.741(16)		
Mn1−O6	2	1.957(8)		
Mn2−O1	2	1.866(8)		
Mn2−O2	1	1.799(15)		
Mn2−O3	1	1.882(16)		
Mn2−O4	2	2.062(8)		
Ca2− O1	4	2.156(6)		
Ca2− O2	2	2.280(11)		
Ca1− O5	1	2.508(13)		
Ca1− O5	1	2.421(12)		
Ca1− O6	2	2.502(7)		
Ca1− O6	2	2.266(8)		
Ca1− O7[a]	2	2.768(27)		
Ca1− O8[a]	1	2.52(4)		
Ca1− O8[a]	2	3.003(11)		

[a] O7 and O8 are the oxygen position in the Ca_2O sheets, which are partially occupied ($^1/_4$).

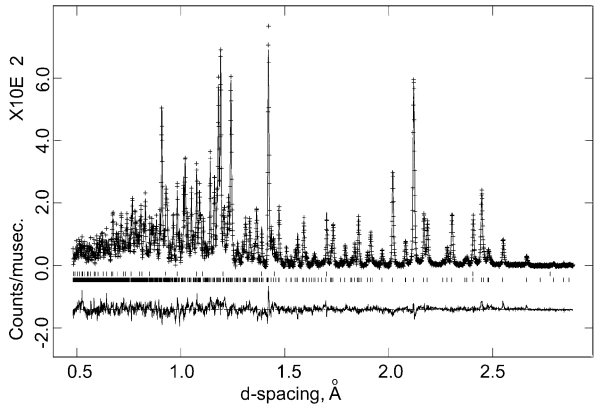

Figure 5. Profile fit of the room-temperature neutron diffraction pattern of $La_4Ba_{2.6}Ca_{1.4}(Mn_4Ca)O_{19}$. The symbol "+" represents the observed pattern, and the solid line represents the calculated pattern; the marks below the pattern indicate the reflection positions of CaO (up) and $La_4Ba_{2.6}Ca_{1.4}(Mn_4Ca)O_{19}$ (down); the difference curve is shown at the bottom of the figure.

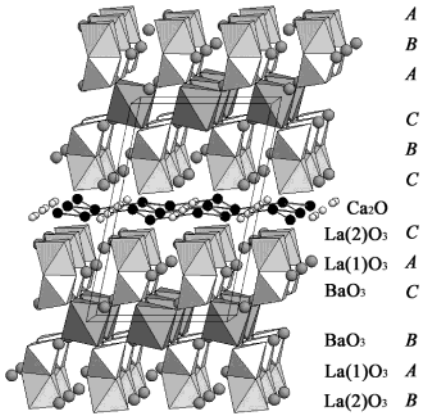

Figure 6. Projection of the structure of $La_4Ba_{2.6}Ca_{1.4}(Mn_4Ca)O_{19}$. The CaO_6 are shown as dark octahedra and the MnO_6 are shown as light octahedra. The A-cations are represented as light circles, and Ca and O atoms in the graphite-like Ca_2O sheets are represented as dark and open circles, respectively. The close-packed AO_3 layers are labeled with *italic* letters on the right.

12) and 2.72 Å (CN = 10), respectively. Clearly, the distribution preference of the La and Ba in the perovskite block is correlated with the difference in cationic size. In this sense, the structure of $La_4Ba_{2.6}Ca_{1.4}(Mn_4Ca)O_{19}$ exemplifies the flexibility of the perovskite-based structure in accommodating mixed metal cations of rather different sizes in the same oxygen polyhedron.

The 6H-hexagonal perovskite blocks are separated by Ca_2O sheets. The Ca atoms in the Ca_2O sheet form a graphite-like net as shown in Figure 7. Additional oxygen atoms (O7 and O8) are present around the center of the hexagon showing a 4-fold distortion. These oxygen positions are partially occupied ($^1/_4$), so that, on average, each Ca-hexagon contains only one oxygen atom. The coordination polyhedron of Ca is a capped trigonal prism as shown in Figure 8. The graphite-like Ca_2O sheet is an essential structural unit in the $A_{n+1}Mn_nO_{3n+3}(Ca_2O)$ series. In the other members, such as $La_2Ca_2MnO_7$ (*n*

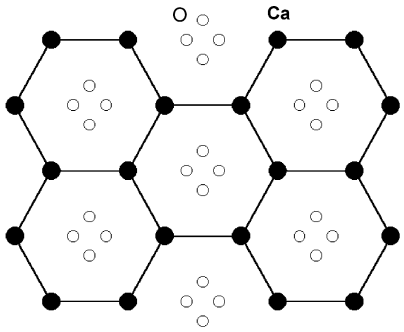

Figure 7. Structure of the graphite-like Ca_2O sheet in $La_4Ba_{2.6}Ca_{1.4}(Mn_4Ca)O_{19}$.

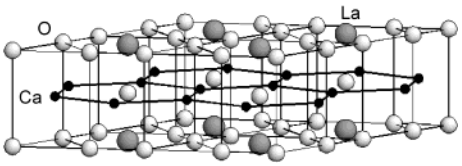

Figure 8. Idealized simple hexagonal packing (***BB***) of close-packed [AO_3] arrays and the trigonal prismatic coordination polyhedra of Ca atoms in the Ca_2O sheet.

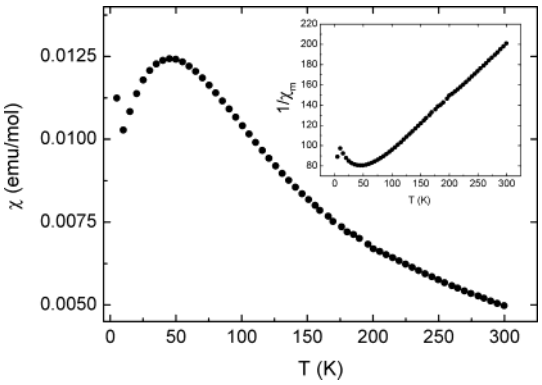

Figure 9. Magnetic susceptibility of $La_4Ba_{2.6}Ca_{1.4}(Mn_4Ca)O_{19}$.

$= 1$),[5] $La_2Ba_{0.8}Sr_{0.6}Ca_{1.6}Mn_2O_{10}$,[6] and $Ba_5Ru_2O_{10}$ ($n = 2$),[8] the Ca_2O sheets exhibit a regular graphite-like symmetry, and the oxygen atoms exhibit a 6-fold distortion according to the higher symmetry of the structures. In the $La_4Ba_{2.6}Ca_{1.4}(Mn_4Ca)O_{19}$, however, the graphite-like Ca_2O sheet is distorted due to the low symmetry. With respect to the family of hexagonal perovskite intergrowth $A_{n+1}Mn_nO_{3n+3}(Ca_2O)$ series, the $La_4Ba_{2.6}Ca_{1.4}(Mn_4Ca)O_{19}$ is an $n = 5$ member in which $^1/_5$ of the Mn atoms in the 6H-hexagonal perovskite blocks are replaced by Ca.

As expected, the $La_4Ba_{2.6}Ca_{1.4}(Mn_4Ca)O_{19}$ is an insulator with conductivity of about 8.1×10^{-7} $\Omega^{1-}cm^{-1}$ at room temperature that increases to about 6.2×10^{-4} $\Omega^{1-}cm^{-1}$ at 680 °C. From the crystal structure, one can see that the Mn−Mn magnetic interaction is mainly within the face-sharing Mn−O octahedral dimer, and the intervening Ca_2O layer would not strongly perturb the localized magnetic character of the Mn^{IV} ions. As shown in Figure 9, the magnetic susceptibility increases with decreasing temperature and reaches a broad maximum at about 45 K. The effective magnetic moment calculated from the high-temperature region is about $\mu_{eff} = 3.4$ B_M, which is comparable to a spin-only isolated Mn^{IV} ionic moment (3.87 B_M). The low-temperature behavior is typical of weak antiferromagnetic interactions between localized manganese ions. The magnetization curves measured at 300, 20, and 10 K do not show significant hysteresis. However, the bending of the magnetization curves at 20 and 10 K may originate from other ferromagnetic impurity or weak ferromagnetic interaction at low temperature. The neutron diffraction at temperatures at about 50 K does not show long-range magnetic ordering of the Mn^{IV} spins.

Discussion

The $A_{n+1}Mn_nO_{3n+3}(Ca_2O)$ structure is formed by alternate stacking of hexagonal perovskite blocks and the graphite-like Ca_2O sheets. The $n = \infty$ end-member corresponds to the $BaNiO_3$-type or the cubic perovskite, and the $n = 0$ end-member corresponds to a hypothetical "ACa_2O_4" structure formed by alternate stacking of single close-packed [AO_3] layers and graphite-like Ca_2O sheets. Between these end members various hexagonal-perovskite intergrowth compounds can be generated systematically. Thus far, three members (i.e., $n = 1$, 2, and 5) have been identified experimentally. The crystallographic data and stacking sequences of these compounds are given in Table 4. All of the known members follow the principle of appropriate stacking of the close-packed [AO_3] arrays and compatible graphite-like sheets. Such a principle is believed to be useful for investigating other unknown members.

Starting from a single hexagonal perovskite layer [A_2MnO_6], denoted as ***AcB***, where the capitals represent the close-packed [AO_3] arrays and the lowercase represents metal atoms in the interstitials, the $n = 1$ member of the series can be built up by adding the close-packed [AO_3] in appropriate sequence. A nontrivial way of adding a subsequent [AO_3] array to the single hexagonal perovskite layer is the simple hexagonal packing (***ABB***), otherwise, for example, ***ABC*** or ***ABA*** would yield only the cubic perovskite or the $BaNiO_3$ structures instead of any new structures. The boundary of (***BB***) layer provides the trigonal prismatic basal plane for cations such as Ca^{2+} to form an adjacent graphite-like net (Figure 8). In the meantime, additional anions are needed in order to separate the opposite A-cations in the [AO_3] layers. The stacking of close-packed layers in the $n = 1$ member could be completed by repeating above sequence either by |***AB***|***BA***| or by |***AB***|***BC***|***CA***|. The structures of these two isomers are similar but different in their unit cells. The former gives rise to a hexagonal cell and the latter forms a trigonal structure with rhombohedral symmetry. The $n = 1$ compound $La_2Ca_2MnO_7$, identified recently within the Ln−Ca−Mn−O systems (Ln = rare earths), crystallizes in an ideal rhombohedral structure of space group $R\bar{3}m$. The structure comprises alternate stacking of single hexagonal perovskite layers and graphite-like Ca_2O sheets as shown in Figure 10a. The stacking sequence of the close-packed [AO_3] follows |***AB***|***BC***|***CA***|. The spatial separation of the close-packed [AO_3] arrays, estimated from this structure, is about 2.25 Å between ***A*** and ***B*** and about 3.52 Å between ***A*** and ***A***. These values could be used to estimate the lattice constants of the other members. Other identified rare earth members such as $Nd_2Ca_2MnO_7$ and $Sm_2Ca_2MnO_7$ form a related distorted structure due to their small cation size (Table 4).

Table 4. Crystallographic Data and Stacking Sequence Regarding the Synthesized Hexagonal Intergrowth Compounds

n	chemical formula	space group	lattice parameters(Å)	stacking sequence	ref
1	$La_2Ca_2MnO_7$	$R\bar{3}m$	$a = 5.62174(4)$, $c = 17.3161(2)$		5
1	$Nd_2Ca_2MnO_7$	$R\bar{3}$	$a = 11.1096(2)$, $c = 17.1987(9)$	$\boldsymbol{A}\vert_c^b\boldsymbol{AcB}\vert_a^c\boldsymbol{BaC}\vert_b^a\boldsymbol{ChA}\vert_c^b\boldsymbol{A}$	6
1	$Sm_2Ca_2MnO_7$	$R\bar{3}$	$a = 11.0428(2)$, $c = 17.1277(5)$		6
2	$La_2Ba_{0.8}Sr_{0.6}Ca_{1.6}Mn_2O_{10}$	$P6_3/mmc$	$a = 5.63591(5)$, $c = 16.2843(3)$	$\boldsymbol{A}\vert_c^b\boldsymbol{AcBcA}\vert_c^b\boldsymbol{AbChA}\vert_c^b\boldsymbol{A}$	7
2	$Ba_5Ru_2O_{11}$	$P6_3/mmc$	$a = 5.9470(5)$, $c = 18.0428(10)$		8
		$R\bar{3}m$ (pseudo-trigonal)	$a = 5.68$, $c = 45.86$		
5	$La_4Ba_{2.6}Ca_{1.4}(Mn_4Ca)O_{19}$	$C2/m$	$a = 9.8394(4)$, $b = 5.6823(2)$ $c = 15.6435(3)$, $\beta = 102.093(5)$	$\boldsymbol{A}\vert_c^b\boldsymbol{AcBcAbCaBaC}\vert_b^a\boldsymbol{ChAbCaBcAcB}\vert_a^c\boldsymbol{BaCaBcAbCbA}\vert_c^b\boldsymbol{A}$	

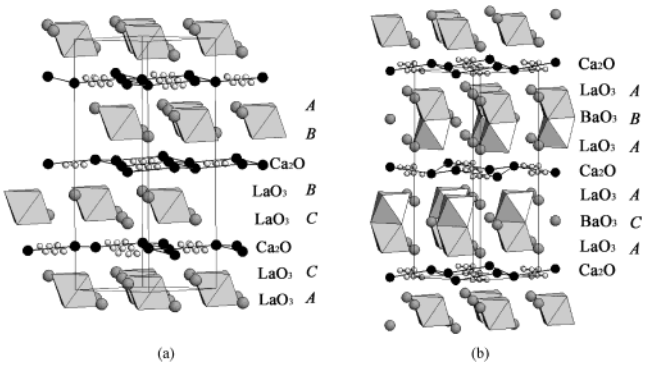

Figure 10. Projection of the structure of (a) $La_2Ca_2MnO_7$ ($n = 1$) and (b) $La_2Ba_{0.8}Sr_{0.6}Ca_{1.6}Mn_2O_{10}$ ($n = 2$). The close-packed AO_3 layers are labeled with *italic* letters on the right.

Similar structure principle can be applied to the other $n > 1$ members in the $A_{n+1}Mn_nO_{3n+3}(Ca_2O)$ family, but the possible isomers will increase dramatically. For $n = 2$, implying two-octahedron thick hexagonal perovskite blocks, the possible stacking sequence might be $|\boldsymbol{ABC}|\boldsymbol{CBA}|$, $|\boldsymbol{ABA}|\boldsymbol{ACA}|$, or $|\boldsymbol{ABA}|$, etc. The octahedra in the first isomer are corner-sharing, resembling the (111) plane of cubic perovskite structure. The latter two isomers, on the other hand, contain face-sharing octahedra grouped in a pair. The structure principle predicts a hexagonal structure and approximate lattice constants of $a = 5.62$ and $c = 16.04$ Å for the first two isomers, and $a = 5.62$ and $c = 8.02$ Å for the third isomer. The two known $n = 2$ compounds, i.e., $La_2Ba_{0.8}Sr_{0.6}Ca_{1.6}Mn_2O_{10}$ and $Ba_5Ru_2O_{10}$ (Table 4), indeed crystallize in a hexagonal structure of space group $P6_3/mmc$ with lattice constants in good agreement with the predicted values. Figure 10b shows the crystal structure of an $n = 2$ member. The structure is formed by alternate stacking of the 2H-hexagonal perovskite blocks and the Ca_2O sheets, and the figure shows a stacking sequence of the second isomer, $|\boldsymbol{ABA}|\boldsymbol{ACA}|$.

For n larger than 2, the number of possible sequences, and hence the number of isomers, increases considerably. For the $n = 5$ compound $La_4Ba_{2.6}Ca_{1.4}(Mn_4Ca)O_{19}$, the stacking sequence can be described as $\boldsymbol{A}|\boldsymbol{ABACBC}|\boldsymbol{CACBAB}|\boldsymbol{BCBACA}|\boldsymbol{A}$, which, under an ideal condition, would crystallize in a trigonal structure with a rhombohedral cell. The cell constants deduced from this packing sequence are $a = 5.62$ and $c = 44.31$ Å, which are very close to those observed from the electron diffraction study ($a = 5.68$, $c = 45.86$ Å). In reality, as discussed above, the structure crystallizes in a C-center monoclinic cell that can be derived directly from the rhombohedral cell by removing the 3-fold axis.

The rapid increase of possible isomers for $n > 2$ renders the aforementioned structure principle limited predictive power of new family members. However, combining the principle with geometric constraints of the perovskite structure such as the well-known Goldschmidt tolerance factor, $t = r_A + r_O/\sqrt{2}\,(r_B + r_O)$ will eliminate many of the unphysical packing sequences. Cubic perovskite is known to be more stable for $0.89 < t < 1$, and the $BaNiO_3$ structure is preferred for $t \geq 1$. In the case of the $n = 2$ member $La_2Ba_{0.8}Sr_{0.6}Ca_{1.6}Mn_2O_{10}$, the B-cation ($Mn^{IV}$, $r_B = 0.67$ Å) and A-cation ($r_A \cong 1.56$ Å) radii impose a tolerance factor $t \cong 1.04$.

Consequently, the packing sequence of |***ABC***|***CBA***| may be disregarded because it gives rise to a small *t* value. In the present case of the $n = 5$ member $La_4Ba_{2.6}Ca_{1.4}(Mn_4Ca)O_{19}$, the mutual substitution of the large and small cations (e.g., Ba and La, as well as Mn and Ca respectively) at a preferred site may complicate the prediction. Nevertheless, the structure principle given above provides a practical means to rationalize the synthesis and to identify the anticipated products from experiments.

In conclusion, we have identified an $n = 5$ member in the $A_{n+1}Mn_nO_{3n+3}(Ca_2O)$ series. $La_4Ba_{2.6}Ca_{1.4}(Mn_4Ca)O_{19}$ crystallizes in a C-centered monoclinic structure, which could be derived from the ideal rhombohedral cell. The structure of this member in conjunction with those of the previously identified $n = 1$ and 2 compounds compile a packing sequencing principle for this family of hexagonal perovskite intergrowth materials. Combined with considerations of other geometric constraints for perovskites, this simple structural principle can be used to predict the variant structures of hexagonal perovskite intergrowth crystals and to guide the synthesis of new compounds in the family.

Acknowledgment. We are thankful for the financial support from NSFC and the State Key Basic Research Program. Work performed at Argonne is supported by US DOE-BES under Contract W-31-109-ENG-38.

Supporting Information Available: Figures of electromagnetic data, magnetization curves, and conductivity of the subject compound. This material is available free of charge via the Internet at http://pubs.acs.org.

CM020706N